AN ABSTRACT OF THE THESIS OF

Andrew M. Abate for the degree of Honors Baccalaureate of Science in Mechanical Engineering presented on May 28, 2014. Title: Preserving the Planar Dynamics of a Compliant Bipedal Robot with a Yaw-Stabilizing Foot Design.

Abstract Approved: _____

Jonathan Hurst

The ATRIAS agile humanoid robot, along with a number of other spring-mass walking machines, currently have two instabilities: one resulting from inertial forces on the torso which cause the robot to spin like a top, and another resulting from stiff ground collisions which cause chattering of the point-contact toes. This thesis presents a solution to these two problems in a manner consistent with the exacting design philosophy of spring-mass walking machines. A passive, compliant, line-contact foot is proposed with only 120 grams of added mass and a fully-adjustable return mechanism.

Key Words: spring-mass walking, SLIP, passive, robot, feet

Corresponding e-mail address: andy.abate@gmail.com

Preserving the Planar Dynamics of a Compliant Bipedal Robot with a Yaw-Stabilizing Foot Design

by

Andrew M. Abate

A PROJECT
submitted to
Oregon State University
University Honors College

in partial fulfillment of
the requirements for the
degree of

Honors Baccalaureate of Science in Mechanical Engineering (Honors Associate)

Presented May 28, 2014
Commencement June 2014

Honors Baccalaureate of Science in Mechanical Engineering project of Andrew M. Abate presented on May 28, 2014.

APPROVED:

Jonathan Hurst, Mentor, representing Mechanical Engineering

Ross Hatton, Committee Member, representing Mechanical Engineering

---

Nancy Squires, Committee Member, representing Mechanical Engineering

---

Dean, University Honors College

I understand that my project will become part of the permanent collection of Oregon State University, University Honors College. My signature below authorizes release of my project to any reader upon request.

Andrew M. Abate, Author

ACKNOWLEDGMENTS

Having spent an absurd amount of time in the Dynamic Robotics Lab, I have a long list of people who have been gracious enough to aid me in my endeavors. First of all, to Jonathan Hurst who gave me the responsibility of designing ATRIAS. To the former senior members of the DRL who showed me many subtleties of the SLIP model and robotics in general, including Alexander Spröwitz and Daniel Renjewski. To the current senior members with whom I share a research space, Christian Hubicki, Hamid Vejdani, Siavash Rezazadeh, Andrew Peekema, and Mikhail Jones. To countless undergraduates and fellow "minions" of the DRL.

CONTENTS

LIST OF FIGURES

LIST OF TABLES

ACRONYMS

CAD Computer-Aided Drafting

CAM Computer-Aided Manufacturing

CNC Computer Numerical Control

COM Center of Mass

DOF Degree of Freedom

DRL Dynamic Robotics Lab

FCA Force Control Actuator

FEA Finite-Element Analysis

FOS Factor of Safety

M3 Maximum Mobility and Manipulation

MIME Mechanical, Industrial, and Manufacturing Engineering

MPRL Machining and Product Realization Lab

SEA Series Elastic Actuator

SLIP Spring Loaded Inverted Pendulum

SLS Selective Laser Sintering

ZMP Zero-Moment Point

1 INTRODUCTION

The field of walking robotics has progressed at an astounding rate over the past two decades; there is a large amount of forward pressure to design humanoid robots which are capable of operating in our very human environment, from simply moving over uneven ground and fitting through doorways, to climbing ladders and driving cars. Recently, the idea of "superhero" robots has become popularized by the DARPA Robotics Challenge[1], where humanoid robots replace humans in dangerous disaster-relief tasks such as search and rescue deep within a burning building, lifting rubble off a trapped citizen, or finding and shutting off a critical valve in an unstable nuclear facility. This is an ideal which researchers are currently working toward, but the humanoid robots that exist right now are a far cry from matching the agility of flesh-and-blood humans. This work is intended to extend the mobility of agile humanoids.

Despite the popular opinion of modern robotics, the field is relatively new and relatively unexplored. Robotics was born after World War II as remote manipulators for handling radioactive material [35], but these were simply rigid mechanisms to begin with, with a mechanical linkage connecting the human-operated controls to the manipulator. The linkages connecting the "master" unit to the "slave" manipulator were eventually replaced with electric circuits and the human operator replaced by an electronic control system. The co-development of Computer Numerical Control (CNC) transformed these remote manipulators into full-fledged robots as we know them today, allowing for pre-programmed trajectories to be followed precisely and repeatably [32]. Naturally, CNC robots like the T3[2] and PUMA[3] found ubiquitous use in assembly lines, where repeatability is critical.

Classical design and control techniques have been applied to walking robots, and they have been proven to be inefficient and vulnerable to disturbances. Several new robots are now utilizing the passive behavior of the mechanism for efficiency and robustness at the hardware level instead of relying solely on control techniques. Due to the model used to design the new "spring-mass" robots, they mostly have point-contact toes, which result in an instability around the yaw axis. Additionally, elastic collisions at the ground cause the toe to chatter, also decreasing stability. To increase the robustness of these robots, a foot needs to be designed which removes sources of instability with surgical precision, without affecting the carefully-planned dynamics of the existing system.

The result of this work is a lightweight, passive foot for the ATRIAS[4] agile running bipedal robots currently located at Oregon State University's Dynamic Robotics Lab (DRL), the University of Michigan's Control Systems Laboratory, and Carnegie Mellon's Robotics

1 The DRC was featured in the Febuary 2013 issue of Popular Science magazine [45].
2 The Tomorrow Tool, 1973
3 Programmable Universal Machine for Assembly, 1978
4 An acronym for "Assume the Robot is a Sphere", referencing the template model under which it is designed.

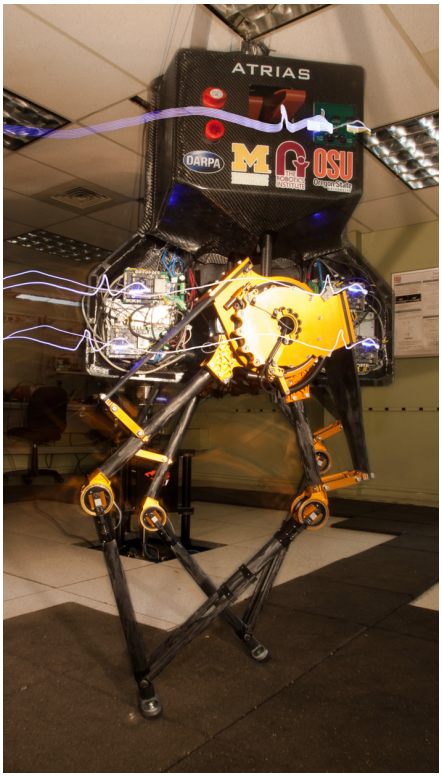

Figure 1: A photo of the ATRIAS humanoid walking.

Institute. ATRIAS is funded by DARPA's Maximum Mobility and Manipulation (M3) program to significantly improve robot mobility and was designed at the DRL by Jonathan Hurst and a team of undergraduate and graduate students, including the author (Figure 1). A single prototype foot was created in fulfillment of the OSU Mechanical, Industrial, and Manufacturing Engineering (MIME) Capstone Design course and tested for effectiveness, then revised for the optimal design.

2 BACKGROUND

The DRL at Oregon State University is currently exploring spring-mass walking with the bipedal robot ATRIAS: a walking, running, agile biped robot designed with efficiency and robustness in mind (Figure 1). These properties are achieved in the *mechanism* of the leg rather than through control policies.

ATRIAS has a rigid torso and two legs, each with three degrees of freedom: leg extension, leg swing, and hip abduction. The legs themselves have two Series Elastic Actuators (SEAs), controlling both the thigh and shin torque relative to the torso, and below which there is a nearly massless carbon fiber leg with a point toe. The springs allow ATRIAS to behave like the Spring Loaded Inverted Pendulum (SLIP) model and follow spring-mass trajectories, which are known to be energetically conservative and highly stable.

The following sections discuss the design philosophy behind ATRIAS, why it needs feet, and why the feet must carefully preserve the purposefully-designed properties which currently exist in ATRIAS.

2.1 CLASSICAL WALKING ROBOTS

Engineers have a great amount of knowledge and experience in the classical form of robotics and control but modern machine-walking research is still having a lot of trouble creating walking robots; it seems that the classical methods we have learned over the last 60 years do not apply when it comes to reproducing the walking and running gaits in animals. Nearly all classically-designed walking machines use what is known as Zero-Moment Point (ZMP) control, where the control system prescribes joint angles and velocities which maintain the overall center of pressure of the robot within its base of support [47] (see [31] for a detailed exploration of classical walking robots). This method has produced robots which are effectively "moving statues", where at any point in time it is perfectly stable. In order to achieve quasi-static stability, the robot must know *exactly* where it is in space and must have an accurate map of the environment, because any unexpected drops will produce large shock-loads on the rigid drive train. Such restrictions amplify the cost of the system and severely limit its region of operation, and it is often the case that classically-designed walking robots cannot run (with the exception of Honda's ASIMO [25]), as that would require an expensive inertial-measurement unit and specialized, high-speed electronics to extrapolate the *exact* moment and velocity of touchdown from the robot's ballistic trajectory, then match the rigid leg's velocity to ground for a soft touchdown. If there is any error in this calculation or the execution of ground-speed matching, there will be a sharp impact force which propagates through the rigid mechanism and could cause damage.

These robots can walk and climb stairs in a stable manner, but they have large energetic costs and are vulnerable to disturbances. ZMP control tends to create level Center of Mass (COM) trajectories which waste energy in the anthropomorphic leg design [29]. Large reflected inertias and rigid links make ZMP robots unsuitable for stable traversal of uncertain terrain. So, what are these robots missing that makes biological systems so flexible?

2.2 ANIMAL LOCOMOTION

Animal motion looks almost effortless when compared to the squat-walking gaits of ZMP machines, so what fundamental properties of animal locomotion can be leveraged to create a more agile machine? Three requirements for robots are clear: mobility, efficiency, and robustness.

2.2.1 *Mobility*

There is a small paradox when considering efficiency in the natural world: engineers consider wheels to be the epitome of efficiency, but animals lack wheels! When it comes to efficiency in nature, the classical argument against animals' evolution of "wheels" as a principal means of locomotion is the problem of transporting nutrients and nerve signals to a continuously-rotating limb. However true this may be, it is far more important to understand that wheels inherently lack mobility [30]; their efficiency is limited to hard, smooth ground. Animals have developed segmented limbs for their versatility, increasing the mobility and fitness the species.

2.2.2 *Efficiency*

Mechanical efficiency of locomotion is very closely tied to the idea of *passive dynamics*: the fundamental dynamics of a system, in absence of any control or actuation. If the "path of least action" [19] coincides with the desired path, then the control system can remain maximally effective, only doing work to counteract frictional losses to heat. Brachiating Gibbon monkeys follow conservative pendular trajectories [46], fish can utilize the energy in vortices to swim upstream at *zero metabolic cost* [7], and kangaroos have extremely efficient tendons to cycle energy in their bounce [5].

It is important that the system not spend calories to remove mechanical energy from its gait when that energy could be conserved and used again. Muscles acting as brakes not only recover *zero* energy, but also *require* metabolic energy. Braking muscles are *doubly avoided* in steady, efficient locomotion for these reasons. This applies to walking robots as well [48]. Walking animals use elasticity in their tendons to conserve and re-use the majority of gait energy [6, 3, 14].

2.2.3 *Robustness*

In natural systems, the line between control and passive dynamics is blurred; the two systems meet at certain points to handle disturbances and maintain stability. Reacting

to disturbances involves much more than "recognizing" that something has occurred, because it has been shown that humans take "action" in response to a disturbance much too fast for that action to have originated from the brain [18]. What appears to be deliberate action in the animal is actually the involuntary and instantaneous motion of the body as a result of favorable passive dynamics in the system. The resulting integrated system is self-stabilized simply due to its passive dynamics [43, 15].

2.2.4 *Application to Walking Robots*

Passive dynamics are considered as the key to efficient[1] walking machines [33, 16]. However efficient, the passive dynamic walkers are extremely limited in mobility (just like wheels), so ATRIAS uses a fundamentally different but equally efficient set of passive dynamics to extend the capability of walking machines.

2.3 MODEL FOR AMBULATION

Giving ATRIAS a useful set of passive dynamics first requires a template model which incorporates efficiency and robustness [20]. Biologists in the 1980s developed the "bouncing ball" model for running, which was formalized as the SLIP [10] and later applied to walking [21]. The SLIP is a template model with a point mass and a massless leg spring, and it can represent any system with a COM, a ground contact, and an effective stiffness between those two points. It has been shown to accurately reproduce the COM trajectory of animals along with the corresponding ground-reaction forces for walking and running [13].

Simulations of this model have shown it to be *inherently stable*, in that a monoped with fixed touchdown angle will take a number of steps before falling [22, 37]. This has a large implication for the field of dynamic walking: even with feedback errors and uncertain terrain, a spring-mass robot can walk or run stably.

One of the realities which is lost on the SLIP model is a rolling center of pressure beneath the foot, which is of great importance in humanoid walking (and other human activities, such as dance). Instead, the SLIP model assumes an immovable point contact with the ground as long as the leg experiences some compression. This fact is important when designing feet for spring-mass walking robots developed from the SLIP model.

2.4 FORCE CONTROL

A new class of compliant manipulators began at MIT with the SEA[2] [38]. This actuator uses a compliant element with a known force-displacement curve in series with a motor to allow for the direct control of forces, where classical systems can only control position. The SEA will assume whatever length is necessary to apply a desired force, whereas classical robots apply whatever force is necessary to reach a desired position. Given that

1 The Cornell Ranger can walk a 40.5 mile ultra-marathon on a closed track [9].
2 also known as a Force Control Actuator (FCA)

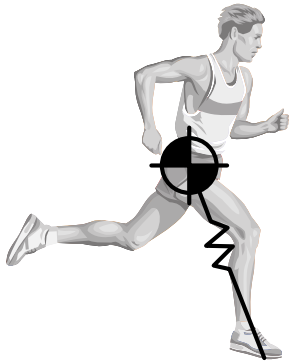

Figure 2: Runner with SLIP template model overlaid. Adapted from [44].

a prime motivation for animal control patterns is to not damage itself, it seems that force control can be heavily applied to walking robotics. ATRIAS incorporates a pair of SEAs to allow for force control in both the leg-length and leg-angle directions.

2.5 NEW PARADIGM FOR WALKING ROBOTS

With the SEA and the SLIP model, several robots have been built with fundamental leg compliance and have experienced positive results (Raibert hoppers [40], resonant hopper [8], self-stabilizing monopod hopper [42], Bow-Leg Hopper [11], ARL Monopod [2], Thumper [27], FastRunner [17], ATRIAS [23, 41, 26]). These robots are energetically conservative and naturally stable due to the spring-in-series design.

2.6 EFFECTS OF A POINT-CONTACT TOE

Most current spring-mass walking robots have point-contact toes as described by their SLIP template model. This is a very physical interpretation of the SLIP model which is reasonable for use in a planar space, but creates instabilities when running in 3D [24].

Currently, ATRIAS is attached to a planarizing boom shown in Figure 3, so it can only walk in a circle. This is enough to test the robot's efficiency and stability [26], as well as prototype optimal controllers, but the ultimate goal for ATRIAS is stable walking and running out in the real world. Preliminary 3D walking results have come from the DRL's sister lab at the University of Michigan, which has an identical copy of ATRIAS, which they call MARLO [12]. These experiments have shown that the momentum of the torso tends to spin ATRIAS around its single point of contact, much like a top[3]. This is a troubling source of instability, and in order to remove it, ATRIAS needs a very special foot: one which restricts the inertial yaw oscillations of the torso while also respecting the very strict requirements of spring-mass walking.

3 See [36] for video.

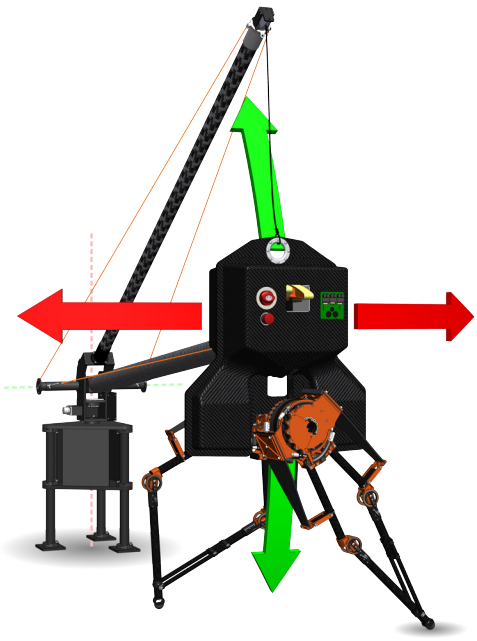

Figure 3: ATRIAS on the planarizing boom. It is constrained to the surface of an imaginary sphere, only able to move in two dimensions.

2.7 EFFECT OF LEG MASS

A physical robot must diverge from the SLIP model in that the leg *will* have mass. (A real-world robot will have a model more similar to a two-mass spring system). This leg mass will experience elastic collisions at the ground, repeatedly breaking and re-establishing ground contact, which is a major source of instability in walking machines. Alexander and Bennett provide a foundational argument for foot pads in animals, where the compliant pads soften ground impacts, decelerate the leg mass, and prevent a loss of ground contact during stance phase (a phenomenon they call "chattering"), and present a simple rule of thumb to prevent this: the foot stiffness must be no more than five times the stiffness of the leg [4]. In addition, a progressive spring will tend to chatter less than a linear spring. Tests performed on human feet [6] and metacarpal foot pads [4] show a stiffening force-deflection curve, substantiating the use of nonlinear foot springs.

2.8 THE NEED FOR FEET

Point-contact toes and leg mass instabilities can both be addressed with the construction of a purposefully-designed foot for spring-mass walking robots, which themselves have subtle designs. To be considered an anchor for the SLIP model, a spring-mass robot must have a COM at the hip, a nearly-massless leg with series compliance, and a free pivot which remains in contact with the ground as long as there is compression in the leg. So, any foot to be added to the robot must adhere to these specifications.

3 PROJECT REQUIREMENTS

Considering the precise assumptions of spring-mass walking machines, the requirements for an accompanying foot should be equally well constructed. Table 1 shows an enumerated list of requirements that must be fulfilled for a dynamically non-destructive foot for spring-mass walking machines. These items stem from assumptions made about the SLIP model, such as zero leg or foot mass, a single fixed point of rotation during stance phase, and no contact during swing phase (reqs. 3, 4, and 5).

A multiple-contact foot (req. 1) is the main motivation of this work, as spring-mass walking machines were designed with perhaps too much focus on the planar SLIP model, neglecting the fact that there is an unstable third Degree of Freedom (DOF) in the yaw direction for point-contact toes. Chatter is another concerning source of instability, so req. 2 seeks to apply some compliance and damping in the same way that animals have foot pads to limit the effect of unsprung mass in the leg.

While ideally these robots could operate without knowing the exact moment of touchdown (taking full advantage of the inherent stability in spring-mass walking), present controllers need a ground-contact signal to know which legs are on the ground (req. 6).

This prototype is designed to fit on the ATRIAS series of robots, which have a standardized coupling on their shins for exactly the purpose of experimenting with new toe and foot designs (req. 7).

The final requirement is listed simply for completeness, and it could otherwise be taken for granted that the foot must be strong enough to not yield under normal operation (req. 8). Failure by yielding within a certain safety factor can be estimated using a Finite-Element Analysis (FEA) software package.

Req	Description
1	Resists disturbance torques in the ground plane (2 DOFs only)
2	Resists chatter
3	Pivots freely at the ground
4	Minimizes distal mass
5	Does not allow ground contact during swing phase
6	Senses ground contact at stance phase
7	Fits on ATRIAS's carbon-fiber shin without any modification to the robot
8	Withstands operational forces

Table 1: List of requirements. Underlines indicate a SLIP assumption which should be very carefully maintained.

4 DESIGN SPACE

The foot design can be separated into three subsystems: foot geometry, contact sensing, and ground clearance. Design variation within each subsystem defines a space of possible solutions which will be explored in this chapter.

4.1 FOOT GEOMETRY

The foot geometry is the overall structure of the foot, including mechanisms, degrees of freedom, and the shape of the footprint. Altogether, the foot for ATRIAS must have exactly two degrees of freedom and no more. With this limitation in mind, consider that there exist only three kind of footprint classified by how many degrees of freedom exist between the foot and the ground under the condition that the foot is fully planted and not sliding. First, point-contact toes can be easily ignored, as they have three degrees of freedom (this is the problem with ATRIAS's original toe!). The two other classes of footprint are line contacts, which have a single degree of freedom, and plane contacts, which cannot move relative to ground. With a planar footprint, two degrees of freedom must be added to the ankle to account for the zero degrees of freedom at the ground contact. This increases the mechanical complexity of the foot and will certainly increase the weight, which should be fervently avoided. This leaves the line contact, which will require only a single ankle DOF to bring the footprint's single DOF up to the required two. This design is like the one employed by Gill and Jerry Pratt's Spring Flamingo [39].

4.2 CONTACT SENSING

There are a great many possibilities to incorporate sensing into the foot in a lightweight manner. The classical approach usually includes a 6-axis force/torque sensor at the foot, but that is overkill for simple contact sensing, they are expensive, and they are heavy.

4.2.1 *Artificial Foot Pad*

Meng Yee Chua and Sangbae Kim prototyped an artificial paw pad, incorporating pressure and other sensors to sense ground contact for the MIT Cheetah quadruped [34]. This technology would be exceptional to include if it were not for the manufacturing difficulty and implementation details.

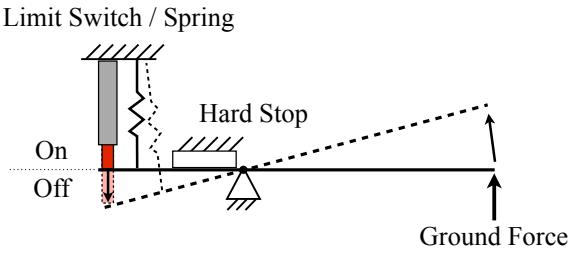

Figure 4: An example momentary-off limit switch for sensing ground contact.

4.2.2 *Ground Profile Sensing*

Kajita and Tani perform full ground profile sensing with an ultrasonic ranger [28]. To sense ground contact, the distance measurement would be compared to some threshold. The same could be done with an infrared optical sensor.

4.2.3 *Absolute Remote Positioning*

A motion-capture system could be used in the lab space to gather accurate position data for ATRIAS and the foot. Small reflective markers would be attached to the foot and identified by an array of video cameras. These video signals would be passed through special motion-tracking software, and the absolute position of the markers within the viewing volume would be returned at discreet moments in time. With the position measurement of multiple markers, the location and orientation of the foot can be found, and the angle of the foot and the height of the ankle can be compared to the ground at that point to determine contact. However, Vicon systems are prohibitively expensive and can only be used in a controlled and static environment.

4.2.4 *Estimated Local Positioning*

To achieve the same position and orientation signal as would be produced by a motion-capture system in a local package, lightweight accelerometer chip can be attached to the foot. However, these sensors tend to drift, requiring some sort of correction [49]. While possible, this method could be too complicated when the only data required is a binary signal of "on" or "off" the ground.

4.2.5 *Direct Contact Sensing*

Limit switches can be a very reliable way to sense contact directly by closing or opening a circuit based on the position of a short-stroke lever or button. This type of sensor should be set up in a momentary-off configuration, where a slight ground contact force actually relieves pressure from the limit switch, allowing it to turn off (Figure 4). This configuration has a large region of "contact" and only a small region of "no contact", whereas a momentary-on configuration has the opposite. Having only a small region of "contact" (the signal we are looking for) will contribute to uncertainty in the measurement. In order to have a limit switch on the foot, it will need an added rigid body moving relative to the main body of the arch, which adds complexity and weight.

4.2.6 *Strain-Based Contact Sensing*

Strain gauges are the most appealing sensor, being steady-state, lightweight, and low-profile. These are small foil resistors which subtly change resistance when stretched, and they can be sensitive enough to measure the strain in metal when properly designed (nearly all force transducers use strain gauges attached to a carefully-designed metal structure). A benefit here could be the incorporation of the sensing element directly into the structure of the foot.

4.3 GROUND CLEARANCE

A design with an ankle DOF will require a return mechanism to maintain a fixed angle during swing phase and prevent oscillations which could cause the robot to trip. It is also possible to have a single-body design with no mechanical degrees of freedom which would not require any reset mechanism.

4.3.1 *Return Spring*

A return spring mechanism requires an adjustable set point for the arch angle relative to the shin, because it is not known exactly how the foot will behave when in operation with various walking or running gaits. It is also necessary to have an adjustable stiffness for the same reason. A very good candidate to serve this function is a simple return spring with damper.

4.3.2 *Single-Body Design*

A design with no mechanical degrees of freedom would always be in an acceptable configuration for touchdown, having only one possible configuration. The robot requires exactly two DOF at the foot, so some cleverness would have to be employed for a single body.

5 POSSIBLE SOLUTIONS AND SELECTED DESIGN

From the design space, two possible designs stand out as acceptable solutions (Figure 5). One has a single DOF with a return spring, while the second is a flexible single-body design with a linear footprint when compressed. For now, the skate design is considered, while the single-body "hoop" is also presented as valid and useful but has too subtle a design to be refined in only a few design iterations.

5.1 POSSIBLE DESIGNS

Strain gauges can be built into almost any structure for ground contact sensing, but the linear footprint limits the design choices for maintaining ground clearance during swing phase. After this narrowing of the design space, only two types of foot present themselves:

5.1.1 *Skate Design*

The skate has a single ankle DOF (plantarflexion, or pitch), which can easily be controlled with a passive return spring. This spring is set so that the foot is parallel with the ground during midstance, maximizing ground clearance for a symmetric gait.

5.1.2 *Hoop Design*

The hoop has zero moving parts, and could fall under the umbrella of soft robotics in the sense that it utilizes the behavior of elastic materials under load. This design has two rolling degrees of freedom, one in the pitch direction and the other in roll. For a rigid body, two rolling DOFs would imply a point contact, but the elastic hoop will flatten and form a line contact with the ground when loaded. This is a very appealing design, but requires a large amount of composites knowledge to get the desired behavior. The heavy downside is that the hoop will have some compliance in the yaw direction, and would have to be carefully designed to minimize that motion.

5.2 SELECTED DESIGN

For reasons of fabrication and assembly, the skate design will be pursued, as the hoop design would be difficult to design a composite structure which has exactly the stiffness properties necessary to be compliant along the leg length but stiff in the yaw direction. This is unfortunate, because a single-body design would reduce complexity and remove the need for a return spring mechanism. However, it is much more likely that the skate design will withstand the punishment of repeated ground impacts on a running machine.

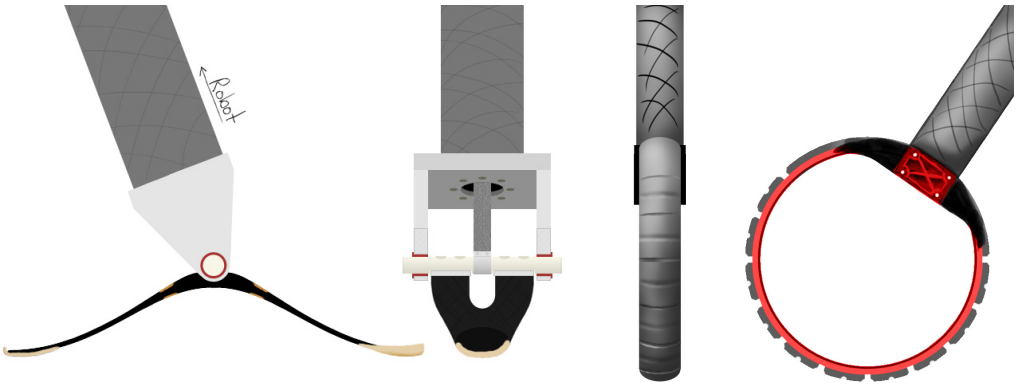

(a) Skate concept. (b) Hoop concept.

Figure 5: Concept sketches.

Also, only the skate design has the facility to be actuated in the future, should it be desired. The full design is shown in Figure 11 with the bill of materials in Table 2.

5.2.1 *Ankle Body*

The body of the foot will have a base, which attaches to the shin of the robot and to two plates which reach down to the ankle joint. These parts designed for 6061 Aluminum stock, which is easy to obtain, but weight reduction features are necessary to bring the mass of the foot to a minimum. For the prototype, weight reduction is not taken as far as it could be, simply to allow for a quick production turnaround. This argument is common for prototyping work.

5.2.2 *Arch*

An arch structure is necessary to support the weight of the robot on the foot pads. It can be analyzed as a two cantilevered beams. The distance between ground contact points was chosen to be symmetric around the ankle axis and arbitrarily six inches apart, simply to have aesthetic proportions with the ATRIAS robot. As a result of these decisions, each cantilever must support 1500 N peak loads at a distance of 75 mm.

The arch was heavily optimized for weight, with a tapered I-beam section to keep stresses constant along the length of the cantilever. FEA was performed in the SolidWorks Computer-Aided Drafting (CAD) package to ensure the stress at any point in the arch is within a safety factor of 2 from the yield strength of 6061-T6 Aluminum. The simulation in Figure 6 shows that the given design has a minimum Factor of Safety (FOS) of 2.2 below the yield strength of 275 MPa.

Because this is a weight-bearing structure, there are large peak forces which require a stiff construction to prevent yielding strains. A strain gauge applied to this stiff structure will have a range from zero to the full load of the robot during running, and the resolution of the signal digitizer will be spread across this range. The controller requires the most sensitivity in the range of zero to ten Newtons, so it is likely that a strain gauge applied to the load-bearing parts of the arch will not be sensitive enough for ground-contact

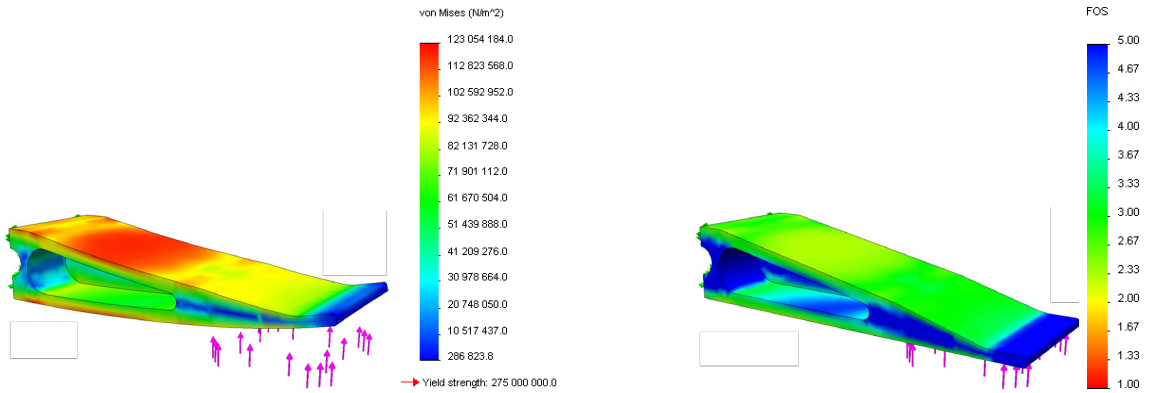

(a) Stress distribution. Max stress is 123 MPa, and yield strength is 275 MPa.

(b) Factor of Safety distribution. Minimum FOS is 2.2.

Figure 6: SolidWorks loading simulation showing von Mises stress and factor of safety in the arch. Symmetric boundary condition at the midsection and distributed load at the pad.

sensing. A more favorable design would have a soft structure for the strain gauge in series with the stiff structure, and the section dedicated to sensing would bottom-out on the load-bearing section to prevent failure of the sensing element. The simple arch design is followed, knowing that a limit switch or slide potentiometer could be easily attached after-the-fact if the strain gauge proves to be useless for contact sensing.

5.2.3 *Ankle Joint*

The ankle joint is the combination of plastic plain bearings and a precision-ground steel shaft, which allows the arch to rotate freely from the ankle body. Igus z-glide flanged bearings provide journal and thrust support with negligible impact on the weight of the foot. These bearings are not completely frictionless, but the small amount of damping they provide will help remove foot oscillations from swing phase without affecting the overall dynamics of the robot.

5.2.4 *Pads*

The pads could possibly be the most important part of the foot, connecting the robot to the ground during stance phase. The pads must have compliance enough to prevent chatter and traction enough to resist yaw torques. One technique which has worked in the past has been a composite fiberglass-urethane skin surrounding a shock absorbing sorbothane pad [1].

The most convenient method of covering sorbothane in a composite skin is to use a simple-curve substrate, in this case a half-cylinder, to allow sheets to be wrapped and layered. Figure 7 shows a cross-section of the foot pad design.

These foot pads are attached to the arch using a small fastener for clamping pressure and a shear pin to firmly hold the pad in place during stance phase. A shear pin is necessary when there are such large shear forces on the ground while running to prevent slipping of the pad beneath fasteners and progressively loosening.

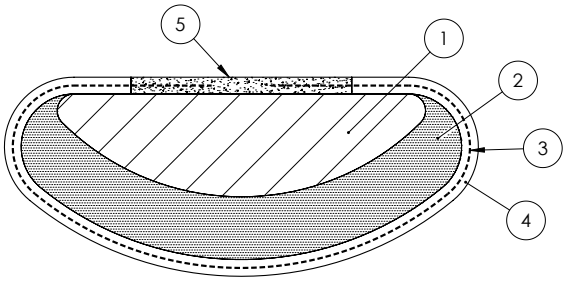

Figure 7: Cross-section of the food pad. (1) Nylon core. (2) Sorbothane layer. (3) Fiberglass weave. (4) Urethane resin encapsulating fiberglass. (5) Epoxy bond holding stitched-together fiberglass in place.

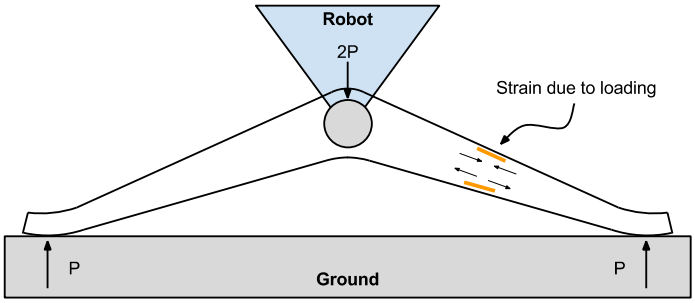

Figure 8: Loading of the symmetric, cantilever foot arch during stance phase and the resulting strain. 2P is the force applied to the foot by the robot. Depending on the motion of the robot, tip loading P may not always be symmetrical.

5.2.5 *Spring Return*

A leaf spring and two clamps create a return mechanism with adjustable set point and adjustable stiffness. The fixed end of the leaf spring is clamped onto the ankle shaft so that it rotates with the arch, and the free end of the spring goes through a slider on the shin. When the arch rotates relative to the shin, this return mechanism will supply a restoring torque in the direction of the set point. To adjust the set point, the base clamp can be loosened and rotated relative to the arch, keeping the spring undeflected. When the base clamp is tightened again, the return mechanism is re-engaged. The stiffness can also be adjusted by using a different leaf spring or moving the sliding joint up or down the shin, changing the effective length of the spring.

5.2.6 *Contact Sensing*

The selected design achieves ground contact sensing in a simple manner, without any added weight or moving parts, by annexing the arch of the foot as a load cell. As shown in Figure 8, the arch is a symmetric cantilever structure, and ground contact can be sensed by measuring the strain due to the loading at its ends.

Four strain gauges are applied to the location of maximum strain on a single cantilever, and the gauges are set up in a full-bridge configuration for maximum sensitivity (Figure 9).

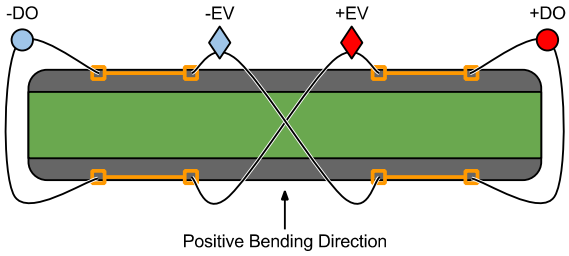

Figure 9: Cross-section of one cantilever showing strain gauge placement. The excitation voltage (EV) and differential output (DO) are the four nodes of the Wheatstone bridge.

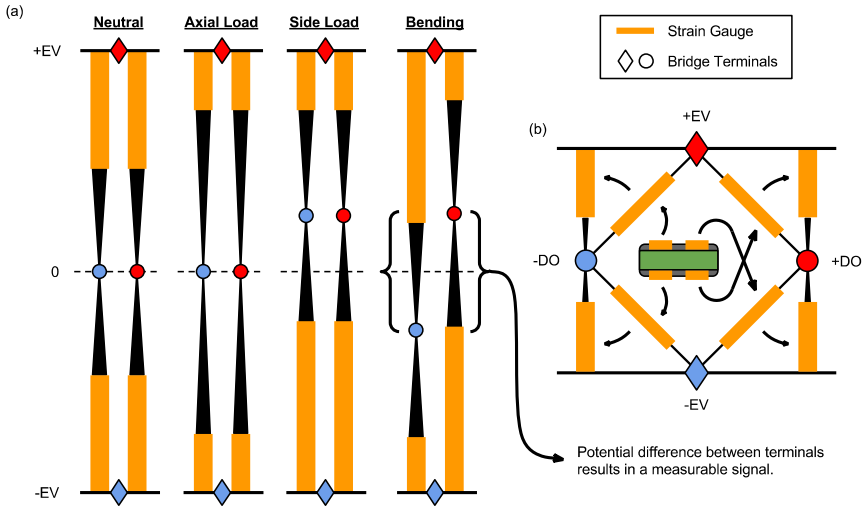

Figure 10: Diagram showing the relationship between electrical and physical properties. (a) The three possible loading modes for the cantilever and the resulting output voltages. The relative length of the strain gauges indicates physical strain. (b) shows how the gauges' geometric placement maps to their location in the Wheatstone bridge.

The Wheatstone bridge has only one output signal and three possible loading modes, so the circuit must be configured so that only one mode results in a signal. To reduce the three inputs to a single output, the desired loading (bending due to ground contact) must result in an antisymmetric voltage change in the bridge's output terminals, and all other loadings must result in a symmetric change. Figure 10 (a) shows how an antisymmetric change in node voltages results in a measurable output signal, while symmetric voltage changes do not register. Bending in the cantilever is geometrically symmetric, so a pair of compressive/tensile gauges must be electrically swapped to create the antisymmetric bridge. The electric position's relation to geometric position can be directly seen in Figure 10 (b), where the gauge cross- section is shown inside the Wheatstone bridge circuit.

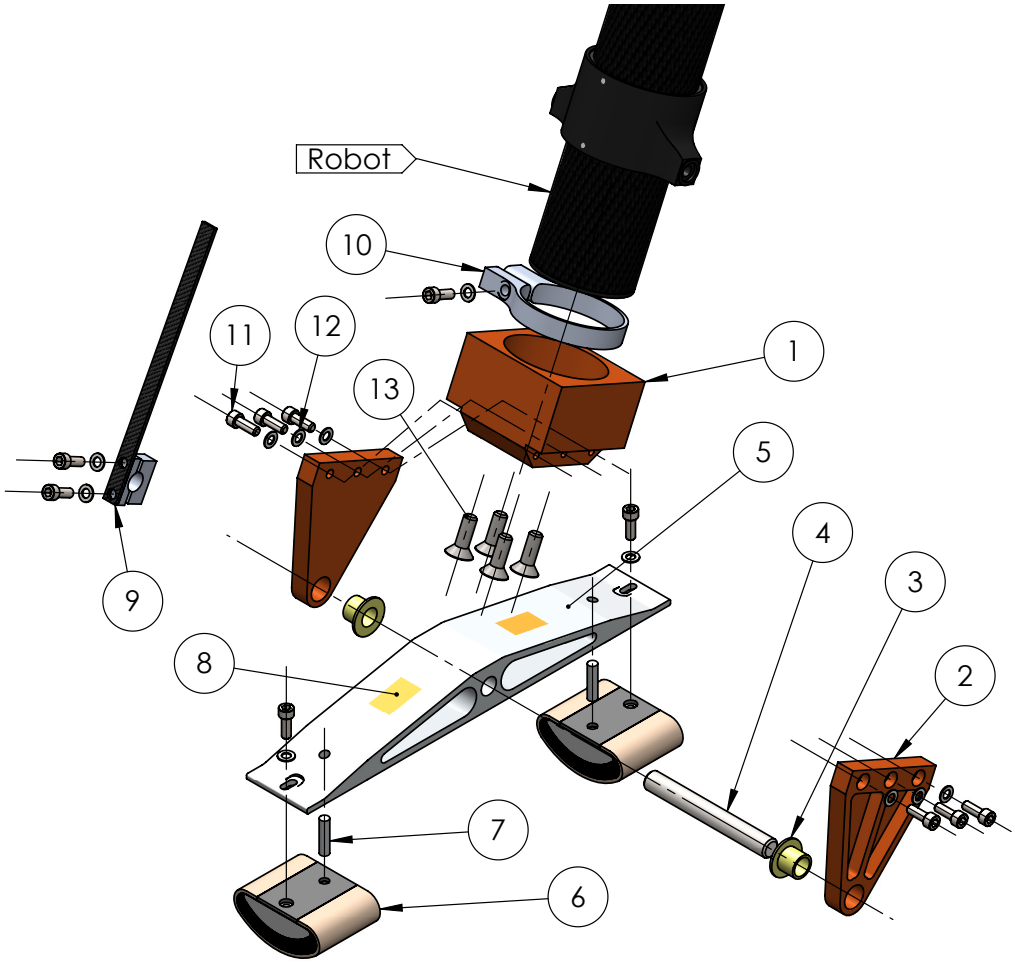

Figure 11: Exploded view of the foot prototype. Part numbers are associated with the bill of materials in Table 2

Table 2: Bill of materials. Part numbers are associated with the exploded view in Figure 11.

#	Part Name	Quantity	Notes
1	Ankle Body	1	Attaches the foot to the shin of the robot.
2	Ankle Plate	2	Bridges the gap between the ankle body and the ankle axis.
3	Plain Bearing	2	Z-glide plastic bearings from Igus are light and small.
4	Ankle Shaft	1	Provides a rotation point and support for the arch.
5	Arch	1	Double-cantilever beam supporting the foot pads.
6a	Pad Half-Cylinder	2	Rigid plastic structure used to build up the foot pad.
6b	Sorbothane Rectangle	2	Pad-like material to prevent chattering.
6c	Skin Rectangle	2	A tough fiberglass-urethane skin to add traction and prevent damage to the pad.
7	Shear Pin	2	Transfers shear force from pad to arch.
8	Strain Gauge	2	Double-linear gauges to be glued to the arch.
9	Spring Clamp	1	Clamps the return spring to the ankle shaft, allowing easy adjustments to the set point.
10	Shin Clamp	1	Anchors the free end of the leaf spring to provide the restoration force when deflected.
11	Cap Screw	11	Used for assembly.
12	Washer	11	Distributes clamping pressure without damaging the parts.
13	Flat-Head Screw	4	Bolts the ankle body to the shin of the robot.

6 MANUFACTURE OF THE SELECTED DESIGN

Once the detail design is completed, the manufacture and assembly of the foot can begin. As discussed in the last chapter, the selected design will include a linear footprint, strain-gauge contact sensing, and a return spring for the single ankle DOF. The SolidWorks CAD package was used to draft the design and produce drawings for manufacture. Toolpaths for a Fadal CNC mill were produced with EdgeCAM, and the prototype was machined in-house. After all parts are ready, the foot prototype can be fully assembled.

6.1 CNC MACHINING

All machined parts were done at the Oregon State University Machining and Product Realization Lab (MPRL) to cut down on costs. Computer-Aided Manufacturing (CAM) was done in the EdgeCAM software package, and toolpaths (in the form of g-code) were generated for the Fadal VMC15 CNC Mill located in the MPRL. The arch and the ankle plates required CNC milling because of their curves and diagonal lines, operations which would be very difficult to do by hand. Each of the two CNC programs needed to be proofed in an easily-machinable material such as wax or foam to make sure there were no collisions or errors. Stock for these parts was ordered from McMaster-Carr's online hardware store or salvaged from waste material of other projects. Figure 12 shows different stages of the milling process.

6.2 SORBOTHANE-FIBERGLASS-URETHANE FOOT PADS

The food pads are constructed layer-by-layer from a plastic half-cylinder, sorbothane sheet, and fiberglass-urethane sheet. A nylon rod is cut in half and the two faces leveled using a fly-cutter in a manual mill. Each half-cylinder has a threaded hole and a hole for a shear pin added. A large swath of fiberglass-urethane sheet is made by laying out the fiberglass with warp and weave fibers at 90° on a flat surface covered in plastic wrap, then saturating it in the urethane. Plastic wrap is laid over the fiberglass and bubbles are worked out with fingers. A flat plate of aluminum is then used as a weight and a way to make the skin a uniform thickness.

To assemble the foot pad, a sorbothane sheet is cut to have the same area as the curved surface of the half-cylinder, and a sheet of the skin material is cut to wrap around the entire perimeter of the foot pad. The sorbothane sheet is glued in place with cyanoacrylate (common "super glue"). The skin material should not be glued to the sorbothane, because that would stiffen the compliant structure, so instead it is sewed together where the ends

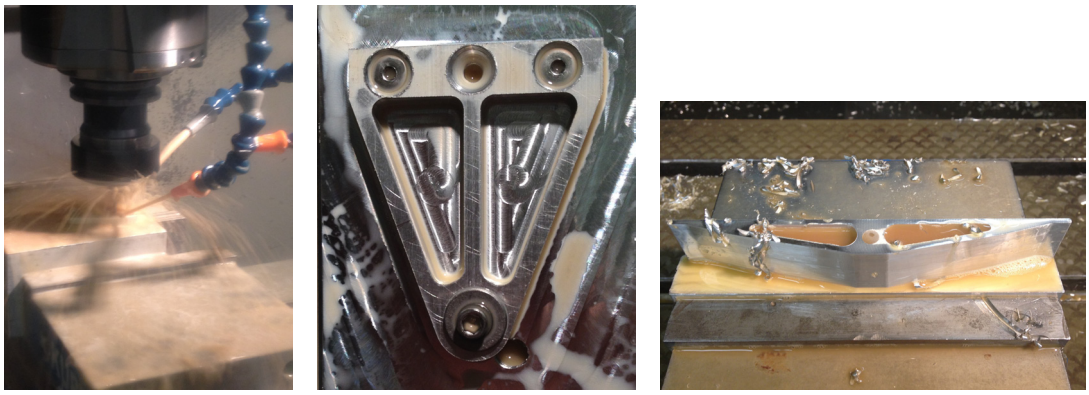

(a) CNC program of ankle plate. (b) Finished ankle plate. (c) Finished arch.

Figure 12: Stages of CNC machining the arch and ankle plates.

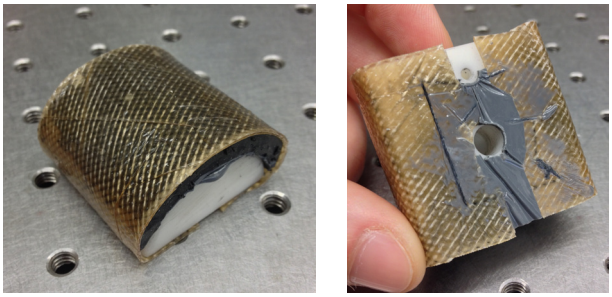

Figure 13: Assembled foot pads. Fibers run diagonally for increased strength.

meet on the flat surface of the half-cylinder and epoxied for a strong and permanent bond. The epoxied assembly is clamped into a mold to imitate the clamping pressure on the skin when the foot pad is attached to the arch; this will give the epoxy a uniform thickness and allow for a good distribution of clamping pressure after the epoxy dries. See Figure 7 for a construction diagram. Figure 13 shows the finished product.

6.3 STRAIN GAUGES

Strain gauges are applied to the arch with cyanoacrylate using a common method, then a two-part epoxy is laid over the gauge for protection. Gluing the gauge to the arch requires acetone, teflon tape, and simple masking tape. The gauge application site is prepped by sanding it down to 400-grid and cleaning with acetone. The gauge is then positioned and a small piece of masking tape is used to secure the short edge opposing the contacts, which acts like a hinge and allows the gauge to be lifted. A small dab of glue is placed at the small edge stuck down with tape, and teflon tape is used to roll the dab of glue along the surface of the gauge and apply pressure necessary to cure the glue without fingers getting stuck as well. After the gauge is glued down, leads are soldered to the gauge's

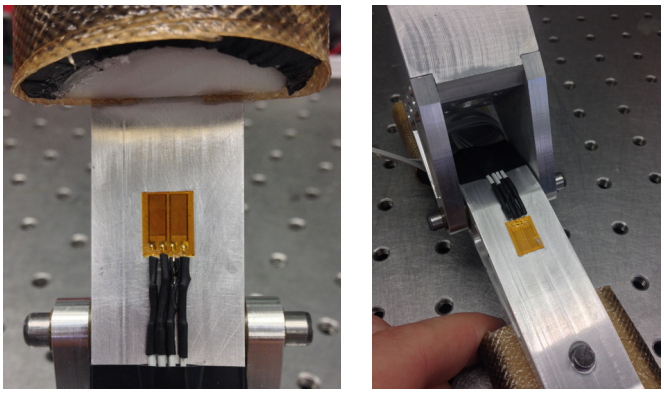

Figure 14: Ground-contact sensing strain gauges after application to arch structure.

terminals and two-part epoxy is applied to protect the gauge and provide strain-relief for the solder joints. Both strain gauges can be seen in Figure 14.

6.4 ASSEMBLY AND FINAL TOUCHES

After the machining process, the arch has large burrs on one side which need to be removed with a file (Figure 15b). When this is done, the foot pads can be clamped onto the arch and the ankle shaft glued in place with Loctite retaining compound. The zglide bearings are pressed into the ankle plates and the arch assembled together with the ankle body. Wires from the strain gauges are routed up to the ankle body and crimped into a connector for easy attachment and removal of the foot from the robot. A flexible carbon fiber return spring is attached, and the foot is now ready for testing.

(a) Immediately after machining.

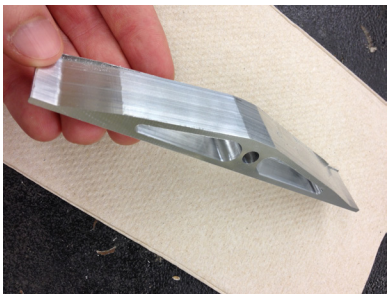

(b) In the process of deburring.

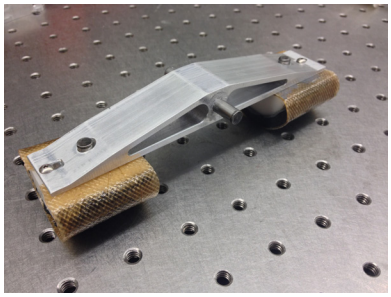

(c) Foot pads added.

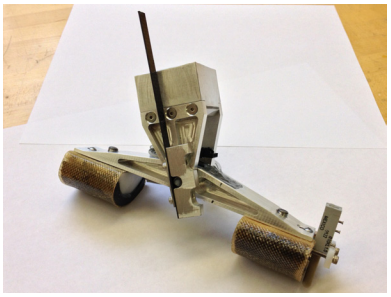

(d) Fully assembled foot.

Figure 15: Stages of foot assembly.

Figure 16: Foot mounted to ATRIAS.

7 FIRST RESULTS

Testing is performed on the foot prototype on the bench (that is, off the robot) so that results can be obtained without regard to which controllers were being run on the robot or the variability in the gait that comes with dynamic walking. Weighing all parts of the completed foot show the total mass to be 280 grams, which is roughly 10% of the total mass of the ATRIAS leg below the springs (2.5 kg, for reference). Mass, return spring stiffness, and stiffness at the ground interface for the prototype foot can be found in Table 3.

Table 3: List of relevant foot properties.

Property	Measurement	Units
Mass	280	g
Ankle Stiffness	0.488	N.m / rad
Ground Contact Stiffness	250	N / mm

7.1 GROUND CONTACT STIFFNESS

The foot's resistance to chatter is measured by comparing the approximate linear stiffness of the arch (including foot pads) to the linearized stiffness of the ATRIAS leg around the average leg length of 90 cm. The stiffness of ATRIAS is known to be 15 N/mm at 90 cm [1], but the stiffness of the foot must be measured using an improvised force-displacement test setup consisting of a bathroom scale, a digital caliper, and a drill press (Figure 17). The scale is placed on the bed of the press with an aluminum plate on top as a rigid datum for measuring displacement, the arch is placed on this datum with the pads facing up, and another flat aluminum plate is mounted in the quill of the press. The arch is then compressed between these two plates, with the force being measured from the scale and the distance between plates being measured with the caliper.

The deflection is then the difference between the zero-force distance between plates and each individual plate separation. This test is shown in Figure 18 with a resulting stiffness of roughly 250 N/mm, which 3.3 times greater than the maximum stiffness of $5 \times 15\,\mathrm{N/mm} = 75\,\mathrm{N/mm}$ recommended by [4].

Simply adding a layer of sorbothane to the pad of the foot is therefore not sufficient to overcome the chattering problem, so all future designs must add further compliance to decrease contact stiffness below 75 N/mm.

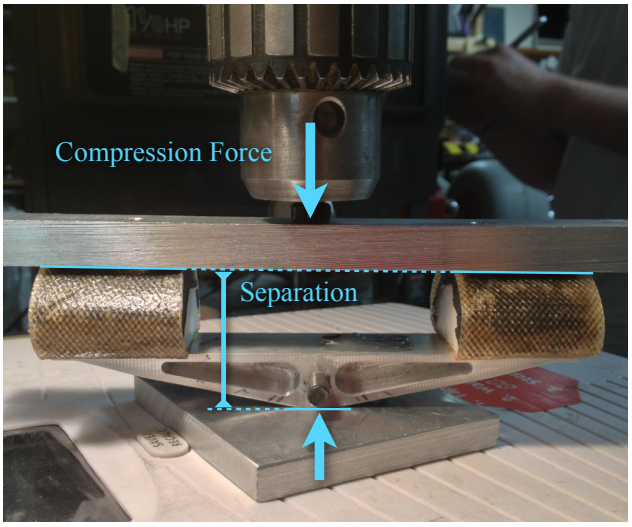

Figure 17: Setup for the ground contact stiffness test. A scale is placed on the bed of a drill press and forces are applied through the quill. Separation of the two datum plates is measured.

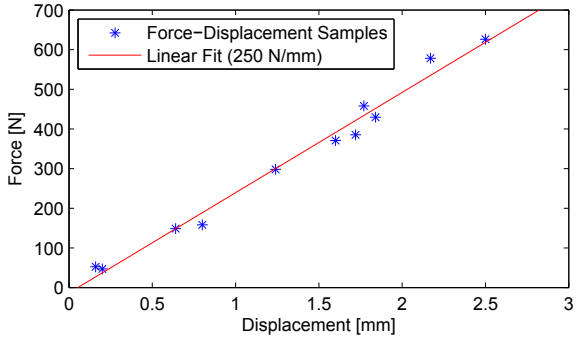

Figure 18: Force-displacement data for the foot showing a nearly-linear relationship for small deflections (3 mm). The resulting stiffness is estimated at 250 N/mm.

7.2 ANKLE STIFFNESS

Torque at various angular deflections is measured to ensure that the resulting disturbance force on the COM of the robot is minimal. The foot is mounted to a fixture, the return spring is put in place, and forces are measured using a torque wrench (Figure 19). Figure 20 shows the torque measured for angles up to 40 degrees. Given that the maximum torque at the ankle is 0.33 N.m, and the lever arm from the ankle to the hip of ATRIAS is exactly one meter, the disturbance force of the foot's return spring is a mere 0.1 pounds. This force is entirely negligible given the 150 pound weight of the robot.

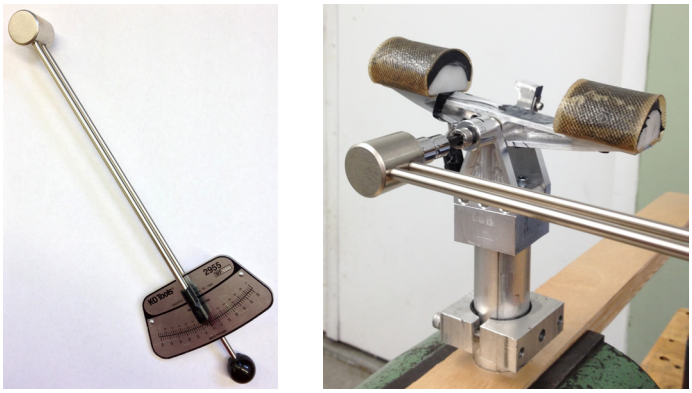

(a) Torque wrench. (b) Foot fixture.

Figure 19: Materials used in ankle stiffness test.

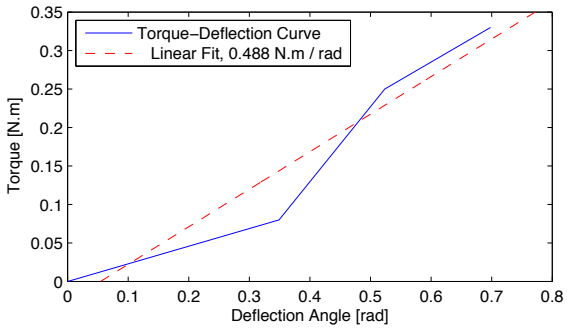

Figure 20: Torque-displacement profile for return spring mechanism.

7.3 YAW STICTION TORQUE

It is principally important that the foot pads maintain a strong contact with the ground to resist inertial yaw torques from the robot, so a test is performed using a forceplate to measure both normal force (ground contact force) and the maximum stiction torque. A jig is created to hold the foot vertical on the forceplate (Figure 21a) and allow the tester to apply normal and twisting forces, which are directly measured by the forceplate. Based on calculations from an average ATRIAS running gait, the foot will need to resist yaw torques of 25 N.m. Figure 21b shows the results of the stiction test, which was terminated when the 25 N.m mark was surpassed.

7.4 SWING PHASE CONTACT TEST

Oscillation natural frequency and damping properties of the foot are characterized and overlaid onto measured foot position data from a real ATRIAS gait to determine ground clearance during swing phase. Angle trajectories of the foot are measured with a linear potentiometer, set up as a voltage divider, attached to LabVIEW through a myDAQ measurement device. The conversion between voltage and angle was done by simply mea-

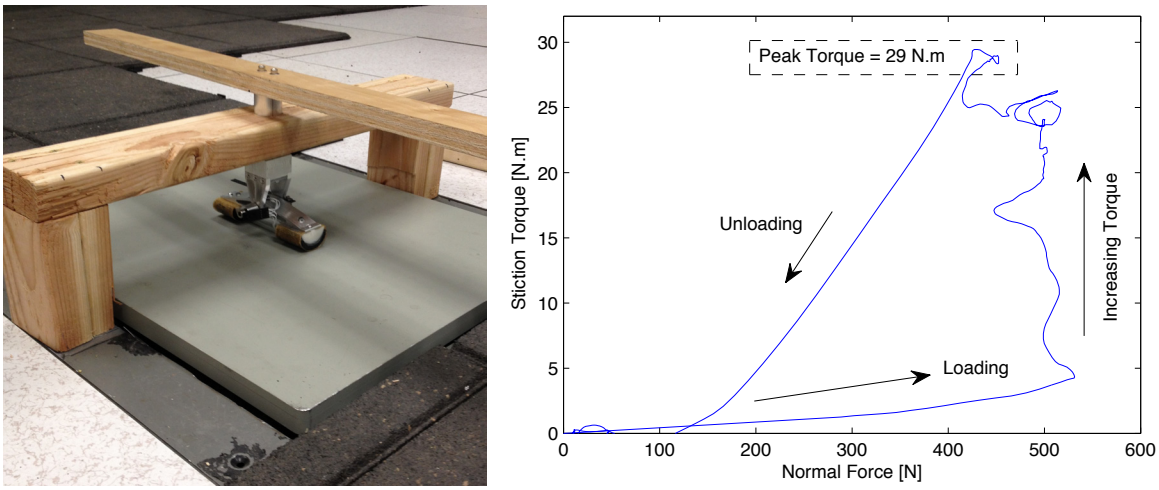

(a) Test setup.

(b) Test results.

Figure 21: Test setup and results for the yaw stiction torque test.

suring the voltage at known angles and deducing the constant of proportionality with $\Delta V/\Delta\theta$. Figure 22 shows the oscillation test setup, in which the foot was "plucked" to excite oscillation. Two impulse responses are shown in Figure 23 along with one step response for variety. These responses were then brought into MATLAB and fit to a general 2nd-order system to determine the damping ratio and natural frequency for which the average measurements were 0.155 and 31.2 rad/s. Because the bearings in the foot are not perfect viscous dampers, as assumed by the 2nd-order model, Coulomb friction will also play a role to stop the oscillation more quickly than estimated, so the given damping ratio will be less than the actual.

When the oscillation of the foot is characterized, a simulated foot can be attached to real robot data to determine if excessive foot oscillation will cause ground contact during swing phase. Figure 24 shows the results of the simulated foot overlaid onto a real ATRIAS gait. The only condition imposed is a foot angle of zero relative to ground when the SLIP point contact is at ground level. There are no collision tests between the foot and ground, it is only important that there is a single heelstrike immediately before foot-flat.

7.5 TESTING SUMMARY

All test performed on the foot prototype meet expectations, except the stiffness of the ground contact, which is too stiff as a result of the aluminum arch and will potentially chatter on touchdown. Swing-phase oscillations of the foot will damp out completely within 400 ms, and simulation results show that the foot will likely not interfere with the robot while in the air. Torque tests also show that the return spring has a negligible impact on the COM trajectory of the robot during stance phase. The composite skin and compliant sorbothane pads give the foot enough traction to resist inertial forces on the robot during running.

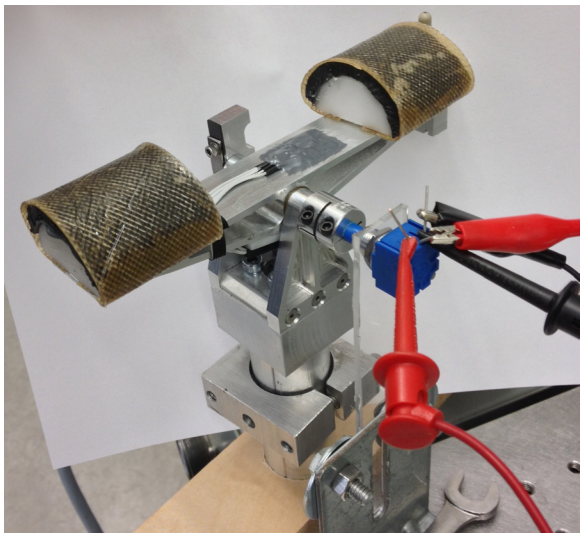

Figure 22: Oscillation test setup. Blue box is a linear potentiometer which is held in place by a sheet of acrylic. Terminal leads go to an excitation voltage and the wiper voltage goes to the measurement device.

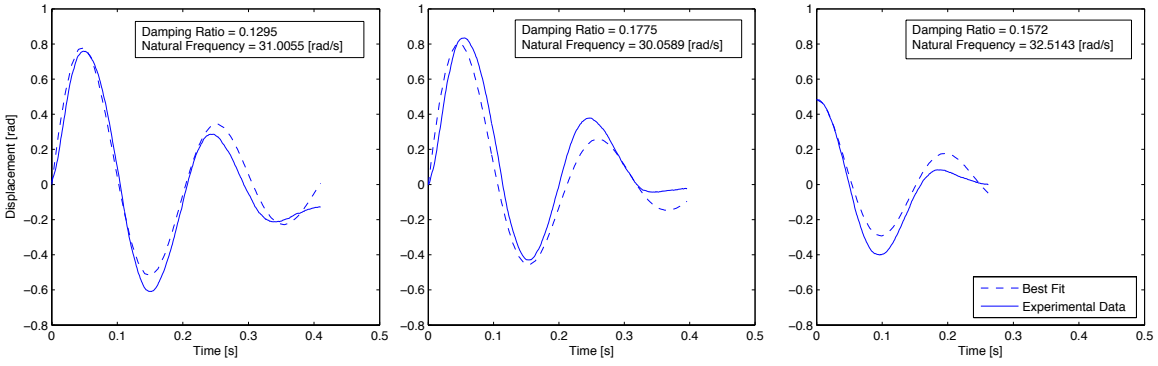

Figure 23: Oscillation test results. Left and middle graphs are impulse responses, and the right graph is a step response. The average damping ratio is 0.155 and the average natural frequency is 31.2 rad/s.

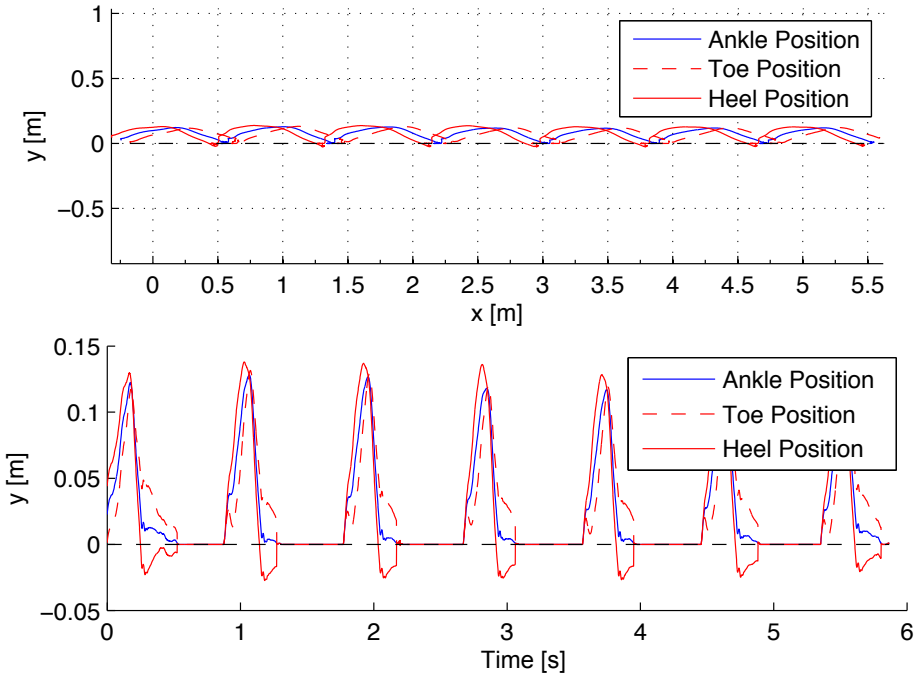

Figure 24: Simulated toe, and heel heights as a function of both time and distance. There is a clear heelstrike before midstance and no contact at all before that. This is a very encouraging result.

8 DESIGN REVISIONS

After testing was complete, it was clear that significant improvements could be made to the design in terms of weight reduction, materials, compliance, and spring-return; the revised design can be seen in Figure 25. It is estimated using the SolidWorks model for the revised design that the weight of each foot can be reduced from 280 grams to 120 grams, and given the time spent on FEA and topology optimization, this seems to be near an absolute minimum for the use of aluminum and fiberglass in a conventional machining process. The body of the foot could potentially be made even lighter using the new Selective Laser Sintering (SLS) technologies becoming widely available to construct more organic, sparse structures (imagine a miniature, three-dimensional network of trusses instead of homogenous aluminum in the ankle body).

8.1 ANKLE BODY

Firstly, the bulk of material on the ankle body and ankle plates (including fasteners) can be removed in favor of an optimized aluminum structure which spans the distance between the robot's shin and the ankle shaft. Weight optimization is limited by the 3-axis milling process, where extra pockets generally require re-fixturing of the workpiece in the mill, so tradeoffs are made between absolute minimum mass and complexity of machining. In the prototype, the bearings had to be shortened to match the thickness of the ankle plates, so this design moves the bearings from the ankle body to the arch body so that the ankle wall can be made minimally thin and still have a large bearing surface in contact with the shaft, which now rotates with the ankle body instead of the arch. This change requires the return mechanism to operate in the small space (literally the wall thickness of the bearings) between the ankle shaft and the arch body. Luckily, the new return mechanism design will benefit from such a tight space.

8.2 RETURN MECHANISM

A magnetic return mechanism is a very convenient way to apply restoring forces to the arch during swing phase, using only passive, internalized components. This mechanism is simply a magnetic dipole immersed in a constant magnetic field (Figure 26); the dipole will have one stable equilibrium position at 0° and one unstable position at 180°. Physically, the dipole is a set of cylinder magnets oriented along the diameter of the ankle shaft, and the constant field is generated by pairs of magnets surrounding the shaft and mounted to the arch body. Attractive forces that exist at the set point and repulsive forces at 180° will drive the arch toward the neutral position, which can be set by loosening

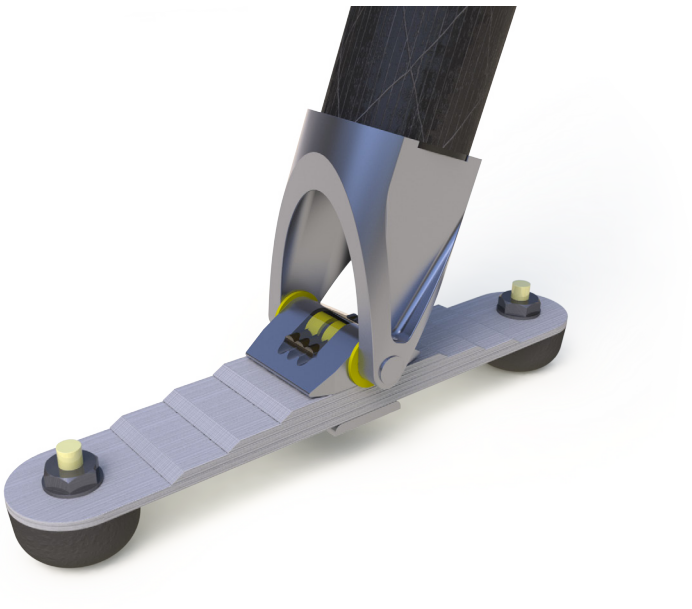

Figure 25: Rendered image of the revised foot design.

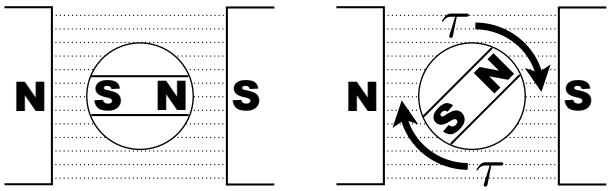

(a) Neutral position. (b) Restoring torques.

Figure 26: A schematic showing the magnetic dipole embedded in the ankle shaft and the constant field attached to the arch.

the set-screws holding the ankle shaft in place and rotating it relative to the body. Even the stiffness can be adjusted by using either more or fewer magnets in the arch body, strengthening or weakening the fixed field. A simple prototype of this mechanism has shown extreme promise.

8.3 COMPLIANT ARCH

The aluminum arch was far too stiff, so the revised design has layers of fiberglass plate which are extremely elastic and rub against each other during deflection, damping out oscillation. Clamping layers of fiberglass to form the arch is highly customizable, so fast iteration can be made on the thickness of layers, types of sheet stock, or even alternating layers of fiberglass and sorbothane for specific stiffness and damping properties.

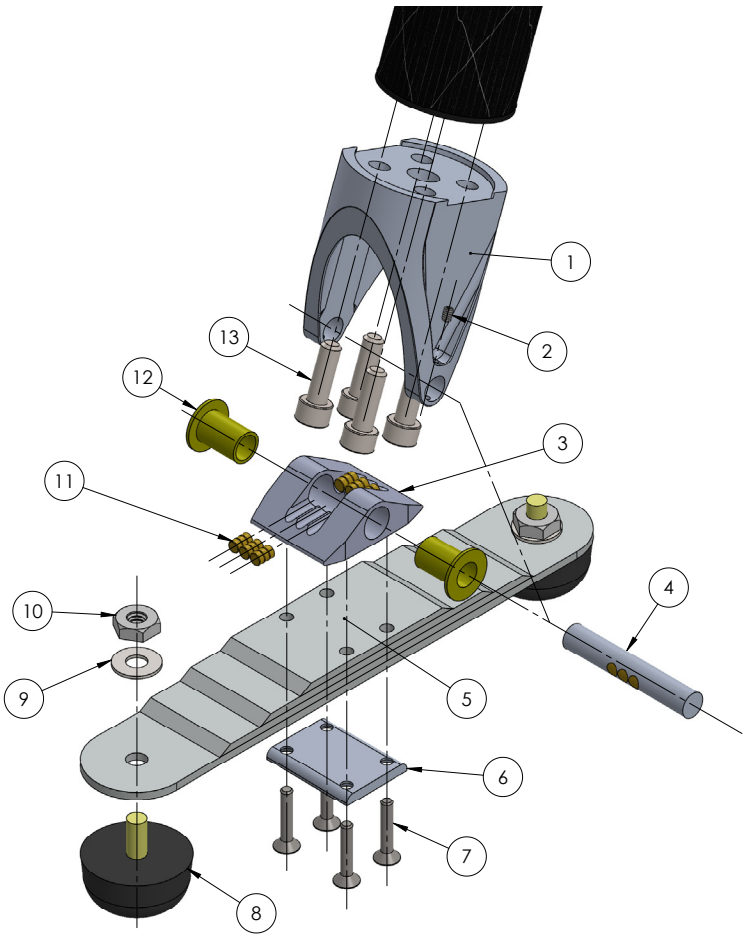

Figure 27: An exploded view of the revised design. Part descriptions are found in Table 4.

8.4 OFF-THE-SHELF PADS

Since the fiberglass arch provides the compliance and damping necessary to prevent chatter, the complex foot pads of the prototype design can be replaced with off-the-shelf neoprene bumpers which can be ordered in bulk. This is a great boon for construction, as the prototype pads could get worn down or damaged and more would have to be made, but the new pre-made bumpers can just be pulled out of a bag.

Table 4: Bill of materials for the revised foot design. An exploded view can be seen in Figure 27.

#	Part Name	Quantity	Notes
1	Ankle Body	1	Attaches the foot to the shin of the robot.
2	Ankle Set Screw	2	Fixes the ankle shaft to the ankle body.
3	Arch Body	1	Rigid structure to support the new fiberglass arch.
4	Ankle Shaft	1	Provides a rotation point and support for the arch. Now includes magnets for the new return mechanism.
5	Fiberglass Arch	1	Layered fiberglass plates provide compliance and damping.
6	Arch Clamp	1	Clamps the layered arch together.
7	Fleat-Head Fastener	4	Clamps the fiberglass layers to the arch body.
8	Neoprene Bumper	2	Stock part from McMaster for easy replacement.
9	Washer	2	Distributes clamping pressure and prevents damage to the fiberglass.
10	Locknut	2	Clamps the bumpers to the fiberglass.
11	Magnet	18	Rare-earth magnets provide a permanent magnetic field for the return mechanism.
12	Plain Bearing	2	Z-glide plastic bearings from Igus are light and small.
13	Cap-Head Screw	4	Bolts the ankle body to the shin of the robot.
14	Strain Gauge	2	Embedded between layers of fiberglass.

9 CONCLUSIONS

Due to the simplistic nature of the SLIP model's point-contact toe and the tendency for spring-mass walking machines to use the same point-contact on the real robot, modern bipedal robots currently have an unstable oscillation of the torso in the yaw direction due to unavoidable inertial forces when walking off-boom and in the three-dimension world. Without a foot, these robots have a tendency to spin like a top around a single point contact. The design of spring-mass walking machines places very narrow restrictions on how their dynamics can be changed, so creating a foot for these machines must be very carefully done to preserve the existing dynamics.

With surgical precision, the foot must permit only two degrees of freedom when in contact with the ground. Principally important is the weight of such a foot, as any added mass negatively affects the robot. Additionally, foot compliance is necessary to prevent ground-contact chatter.

The proposed design is a passive, skate-style foot with a linear footprint and single ankle joint to provide two degrees of freedom at the ground contact. A compliant arch softens the touchdown impact, limiting the chatter effect. An adjustable return mechanism is included to prevent the foot from tripping the robot. After the proposed design was prototyped with a 280 gram mass, revisions to the CAD model brought the mass down to an estimated 120 grams, which is only 4.8% of ATRIAS's unsprung leg mass.

As of this writing, two of the revised feet are being built and will soon be tested on ATRIAS with the DRL's state-of-the-art walking controllers.

BIBLIOGRAPHY

[1] DRL Tribal Knowledge.

[2] M. Ahmadi and M. Buehler. The ARL monopod II running robot: control and energetics. In *1999 IEEE International Conference on Robotics and Automation, 1999. Proceedings*, volume 3, pages 1689–1694 vol.3, 1999. doi: 10.1109/ROBOT.1999.770352.

[3] R. McN. Alexander. Three uses for springs in legged locomotion. *Int. J. Rob. Res.*, 9(2):53–61, 1990. ISSN 0278-3649. doi: 10.1177/027836499000900205. URL http://dx.doi.org/10.1177/027836499000900205.

[4] R. McN. Alexander and M. B. Bennett. Mechanical properties and function of the paw pads of some mammals. *Journal of Zoology*, 209(3):405–419, 1986.

[5] R. McN. Alexander and Alexandra Vernon. The mechanics of hopping by kangaroos (macropodidae). *Journal of Zoology*, 177(2):265–303, October 1975. ISSN 1469-7998. doi: 10.1111/j.1469-7998.1975.tb05983.x. URL http://onlinelibrary.wiley.com/doi/10.1111/j.1469-7998.1975.tb05983.x/abstract.

[6] R. McNeill Alexander. *Elastic mechanisms in animal movement*. Cambridge University Press, Cambridge [England] ; New York, 1988. ISBN 0521341604.

[7] D. N. Beal, F. S. Hover, M. S. Triantafyllou, J. C. Liao, and G. V. Lauder. Passive propulsion in vortex wakes. *Journal of Fluid Mechanics*, 549(-1):385, 2006. ISSN 0022-1120, 1469-7645. doi: 10.1017/S0022112005007925. URL http://www.journals.cambridge.org/abstract_S0022112005007925.

[8] M.D. Berkemeier and K.V. Desai. Design of a robot leg with elastic energy storage, comparison to biology, and preliminary experimental results. In , *1996 IEEE International Conference on Robotics and Automation, 1996. Proceedings*, volume 1, pages 213–218 vol.1, April 1996. doi: 10.1109/ROBOT.1996.503597.

[9] Pranav A. Bhounsule, Jason Cortell, and Andy Ruina. Design and control of ranger: an energy-efficient, dynamic walking robot. In *Proc. CLAWAR*, pages 441–448, 2012. URL http://books.google.com/books?hl=en&lr=&id=0RRGzVpGjB4C&oi=fnd&pg=PA441&dq=%22steering+mechanism+that+enables+turning+of+this+essentially+planar+robot,%22+%22walkers5+but+fall+down+frequently,+or+like+PETMAN,1+BigDog,6%22+%221.+(a)+Ranger.+(b)+2D+schematic.+The+fore-aft+cylinders+with+%E2%80%98eyes%E2%80%99+and+the%22+&ots=mlGdOJZr-p&sig=D2aw4ta_mWVg3wNXrvvdLeQemV4.

[10] R Blickhan. The spring-mass model for running and hopping. *J Biomech*, 22(11-12):1217–1227, 1989. ISSN 0021-9290. PMID: 2625422.

[11] B. Brown and G. Zeglin. The bow leg hopping robot. In *1998 IEEE International Conference on Robotics and Automation, 1998. Proceedings*, volume 1, pages 781–786 vol.1, May 1998. doi: 10.1109/ROBOT.1998.677072.

[12] Brian G. Buss, Alireza Ramezani, Kaveh Akbari Hamed, Brent A. Griffin, Kevin S. Galloway, and Jessy W. Grizzle. Preliminary walking experiments with underactuated 3D bipedal robot MARLO. 2014. URL http://web.eecs.umich.edu/~grizzle/papers/IROS2014_Buss_Grizzle.pdf.

[13] G. A. Cavagna, F. P. Saibene, and R. Margaria. Mechanical work in running. *Journal of Applied Physiology*, 19(2):249–256, 1964. ISSN 8750-7587, 1522-1601. URL http://jap.physiology.org/content/19/2/249.

[14] G. A. Cavagna, N. C. Heglund, and C. R. Taylor. Mechanical work in terrestrial locomotion: two basic mechanisms for minimizing energy expenditure. *American Journal of Physiology - Regulatory, Integrative and Comparative Physiology*, 233(5):R243–R261, November 1977. ISSN 0363-6119, 1522-1490. URL http://ajpregu.physiology.org/content/233/5/R243.

[15] Te-yuan Chyou. *Passive dynamics in animal locomotion*. PhD thesis, University of Otago, 2012. URL http://otago.ourarchive.ac.nz/handle/10523/2663.

[16] S. Collins. Efficient bipedal robots based on passive-dynamic walkers. *Science*, 307 (5712):1082–1085, February 2005. ISSN 0036-8075, 1095-9203. doi: 10.1126/science.1107799. URL http://www.sciencemag.org/cgi/doi/10.1126/science.1107799.

[17] S. Cotton, I.M.C. Olaru, M. Bellman, T. van der Ven, J. Godowski, and J. Pratt. FastRunner: a fast, efficient and robust bipedal robot. concept and planar simulation. In *2012 IEEE International Conference on Robotics and Automation (ICRA)*, pages 2358–2364, May 2012. doi: 10.1109/ICRA.2012.6225250.

[18] Monica A. Daley. Biomechanics: Running over uneven terrain is a no-brainer. *Current Biology*, 18(22):R1064–R1066, November 2008. ISSN 0960-9822. doi: 10.1016/j.cub.2008.09.050. URL http://www.sciencedirect.com/science/article/pii/S0960982208012803.

[19] Richard Phillips Feynman, Robert B. Leighton, and Matthew Linzee Sands. The feynman lectures on physics. 1963. URL http://www.bcin.ca/Interface/openbcin.cgi?submit=submit&Chinkey=125862.

[20] R. J. Full and D. E. Koditschek. Templates and anchors: neuromechanical hypotheses of legged locomotion on land. *Journal of Experimental Biology*, 202(23):3325–3332, December 1999. ISSN 0022-0949, 1477-9145. URL http://jeb.biologists.org/content/202/23/3325. PMID: 10562515.

[21] H. Geyer, A. Seyfarth, and R. Blickhan. Compliant leg behaviour explains basic dynamics of walking and running. *Proceedings of the Royal Society B: Biological Sciences*, 273(1603):2861–2867, November 2006. ISSN 0962-8452, 1471-2954. doi: 10.1098/rspb.2006.3637. URL http://rspb.royalsocietypublishing.org/cgi/doi/10.1098/rspb.2006.3637.

[22] Hartmut Geyer, Reinhard Blickhan, and Andre Seyfarth. Natural dynamics of spring-like running: Emergence of selfstability. In *5th International Conference on Climbing and Walking Robots*, volume 92. Sufolk, England: Professiona l Engineer ing Publishing Ltd, 2002. URL http://lauflabor.ifs-tud.de/files/papers/clawar02_Geyer.pdf.

[23] Jesse A. Grimes and Jonathan W. Hurst. The design of atrias 1.0 a unique monopod, hopping robot. In *International Conference on Climbing and Walking Robots*, 2012. URL http://mime.oregonstate.edu/research/drl/publications/_documents/grimes_2012a.pdf.

[24] Kaveh Akbari Hamed and Jessy W. Grizzle. Event-based stabilization of periodic orbits for underactuated 3-d bipedal robots with left-right symmetry. 2013. URL http://ieeexplore.ieee.org/xpls/abs_all.jsp?arnumber=6663683.

[25] Honda Public Relations Division. ASIMO: the honda humanoid robot, techinical information. Technical report, Honda Motor Co., Ltd, 2007. URL http://asimo.honda.com/downloads/pdf/asimo-technical-information.pdf.

[26] Christian Hubicki, Jesse Grimes, Mikhail Jones, Daniel Renjewski, Alexander Spröwitz, Andy Abate, and Jonathan Hurst. ATRIAS: enabling agile biped locomotion with a template-driven approach to robot design. *IJRR*, 2014 (Currently under review).

[27] Jonathan Hurst and Alfred Rizzi. Series compliance for an efficient running gait. *IEEE Robotics & Automation Magazine*, 15(3):42–51, 2008. ISSN 1070-9932. doi: 10.1109/MRA.2008.927693. URL http://ieeexplore.ieee.org/lpdocs/epic03/wrapper.htm?arnumber=4624582.

[28] Shuuji Kajita and Kazuo Tani. Adaptive gait control of a biped robot based on realtime sensing of the ground profile. *Autonomous Robots*, 4(3):297–305, 1997. URL http://link.springer.com/article/10.1023/A:1008848227206.

[29] A. D. Kuo. Choosing your steps carefully. *Robotics & Automation Magazine, IEEE*, 14(2):18–29, 2007. URL http://ieeexplore.ieee.org/xpls/abs_all.jsp?arnumber=4264364.

[30] Michael LaBarbera. Why the wheels won't go. *The American Naturalist*, 121(3):395–408, March 1983. ISSN 0003-0147. URL http://www.jstor.org/stable/2461157.

[31] Sebastian Lohmeier. *Design and realization of a humanoid robot for fast and autonomous bipedal locomotion*. PhD thesis, Verl. Dr. Hut, München, 2010.

[32] J. Y S Luh, M. W. Walker, and R. P C Paul. Resolved-acceleration control of mechanical manipulators. *IEEE Transactions on Automatic Control*, 25(3):468–474, June 1980. ISSN 0018-9286. doi: 10.1109/TAC.1980.1102367.

[33] Tad McGeer. Passive dynamic walking. *The International Journal of Robotics Research*, 9(2):62–82, 1990. ISSN 0278-3649, 1741-3176. doi: 10.1177/027836499000900206. URL http://ijr.sagepub.com/content/9/2/62.

[34] Meng Yee Chuah. Composite force sensing foot utilizing volumetric displacement of a hyperelastic polymer. Master's thesis, MIT, 2012.

[35] Richard M. Murray. *A mathematical introduction to robotic manipulation*. CRC Press, Boca Raton, 1994. ISBN 0849379814.

[36] University of Michigan News. Two-legged robot walks outside at u-michigan. URL http://ns.umich.edu/new/multimedia/videos/21849-two-legged-robot-walks-outside-at-u-michigan.

[37] Frank Peuker, Christophe Maufroy, and André Seyfarth. Leg-adjustment strategies for stable running in three dimensions. *Bioinspiration & Biomimetics*, 7 (3):036002, 2012. ISSN 1748-3182, 1748-3190. doi: 10.1088/1748-3182/7/3/036002. URL http://stacks.iop.org/1748-3190/7/i=3/a=036002?key=crossref.9eb9b428ad0880a48b8522517c9c9e09.

[38] Gill Pratt and Matthew Williamson. *Series Elastic Actuators*. IEEE Computer Society Press, Los Alamitos, Calif, 1995. ISBN 0818671084.

[39] Jerry E. Pratt and Gill A. Pratt. Exploiting natural dynamics in the control of a planar bipedal walking robot. In *PROCEEDINGS OF THE ANNUAL ALLERTON CONFERENCE ON COMMUNICATION CONTROL AND COMPUTING*, volume 36, pages 739–748. UNIVERSITY OF ILLINOIS, 1998. URL ftp://theory.csail.mit.edu/pub/users/jpratt/natural_dynamics.pdf.

[40] Marc H. Raibert. Legged robots. *Communications of the ACM*, 29(6):499–514, 1986. URL http://dl.acm.org/citation.cfm?id=5950.

[41] Alireza Ramezani and JW Grizzle. ATRIAS 2.0, a new 3D bipedal robotic walker and runner. In *Proceedings of the 2012 International Conference on Climbing and walking Robots and the Support Technologies for Mobile Machines*, pages 467–474, 2012.

[42] R. Ringrose. Self-stabilizing running. In , *1997 IEEE International Conference on Robotics and Automation, 1997. Proceedings*, volume 1, pages 487–493 vol.1, April 1997. doi: 10.1109/ROBOT.1997.620084.

[43] T. J. Roberts and E. Azizi. Flexible mechanisms: the diverse roles of biological springs in vertebrate movement. *Journal of Experimental Biology*, 214(3):353–361, 2011. ISSN 0022-0949, 1477-9145. doi: 10.1242/jeb.038588. URL http://jeb.biologists.org/cgi/doi/10.1242/jeb.038588.

[44] W. J. Schwind and D.E. Koditschek. Approximating the stance map of a 2-DOF monoped runner. *Journal of Nonlinear Science*, 10(5):533–568, 2000. ISSN 0938-8974, 1432-1467. doi: 10.1007/s003320010001. URL http://repository.upenn.edu/cgi/viewcontent.cgi?article=1442&context=ese_papers.

[45] Erick Sofge. How to build a hero. *Popular Science*, Febuary 2013. URL http://www.popsci.com/technology/article/2013-01/how-build-hero.

[46] J. R. Usherwood. Understanding brachiation: insight from a collisional perspective. *Journal of Experimental Biology*, 206(10):1631–1642, 2003. ISSN 00220949, 14779145. doi: 10.1242/jeb.00306. URL http://jeb.biologists.org/cgi/doi/10.1242/jeb.00306.

[47] Miomir Vukobratović and Branislav Borovac. Zero-moment point—thirty five years of its life. *International Journal of Humanoid Robotics*, 1(01):157–173, 2004. URL http://www.worldscientific.com/doi/abs/10.1142/S0219843604000083.

[48] K. J. Waldron and G. L. Kinzel. The relationship between actuator geometry and mechanical efficiency in robots. *Fourth, _'mposium on Theory and Practice of Robots and Manipulators. Poland*, 1981.

[49] Xiaoping Yun, Eric R. Bachmann, Hyatt Moore, and James Calusdian. Self-contained position tracking of human movement using small inertial/magnetic sensor modules. In *Robotics and Automation, 2007 IEEE International Conference on*, pages 2526–2533. IEEE, 2007. URL http://ieeexplore.ieee.org/xpls/abs_all.jsp?arnumber=4209463.

COLOPHON

This document was typeset using the typographical look-and-feel `classicthesis` developed by André Miede. The style was inspired by Robert Bringhurst's seminal book on typography *"The Elements of Typographic Style"*. `classicthesis` is available for both LaTeX and LyX:

http://code.google.com/p/classicthesis/

Final Version as of May 29, 2014 (`classicthesis` 4.1).

UNIVERSITY HONORS COLLEGE COPYRIGHT RELEASE FORM

We are planning to release this Honors Thesis in one or more electronic forms. I grant the right to publish my thesis entitled, Preserving the Planar Dynamics of a Compliant Bipedal Robot with a Yaw-Stabilizing Foot Design in the Honors College OSU Library's Digital Repository (D-Space), and its employees the nonexclusive license to archive and make accessible, under conditions specified below.

The right extends to any format in which this publication may appear, including but not limited to print and electronic formats. Electronic formats include but are not limited to various computer platforms, application data formats, and subsets of this publication.

I, as the Author, retain all other rights to my thesis, including the right to republish my thesis all or part in other publications.

I certify that all aspects of my thesis which may be derivative have been properly cited, and I have not plagiarized anyone else's work. I further certify that I have proper permission to use any cited work which is included in my thesis which exceeds the Fair Use Clause of the United States Copyright Law, such as graphs or photographs borrowed from other articles or persons.

Corvallis, Oregon, May 28, 2014

Andrew M. Abate